Astron. Astrophys. 187, 543–550 (1987)

ASTRONOMY AND ASTROPHYSICS

# Spectrophotometry of comet P/Halley

## I. Flux, column density and emission gradients within the coma in the emission bands and the continuum

**K.R. Sivaraman, G.S.D. Babu, B.S. Shylaja, and R. Rajamohan**

Indian Institute of Astrophysics, Bangalore 560034, India

Received March 4, accepted July 15, 1987

**Summary.** We have made spectral scans of comet P/Halley using the scanner at the Cassegrain focus ($f/13$) of the 102 cm reflector at Kavalur. The scans cover generally the wavelength region from 3900 to 6200 Å and are at 40 Å resolution and on a few occasions in the blue region at 20 Å resolution. The $f/13$ beam provided an image of the coma with a scale of 15″.5 $mm^{-1}$. We have obtained scans on several consecutive nights in March and April, 1986 with a 25″.9 entrance aperture of the scanner at discrete and systematically displaced locations within the coma in the anti-sunward direction as well as normal to it about the position of the nucleus. We have derived the brightness profiles of the neutrals and dust within the coma and have discussed the variations of the spatial gradients of the profiles.

**Key words:** spectrophotometry of comet P/Halley – spatial distribution of gas and dust

### 1. Introduction

Spectrophotometric measurements of fluxes in the emission bands of the different radicals in the neutral atmospheres of comets constitute the principal diagnostics for understanding the origin, behaviour and the chemical composition of these species in the environment of cometary comae. The law governing the heliocentric dependence of the flux in the emission bands provides clues to the volatility of the snows. Furthermore, if emission profiles of the various radicals are secured at independent locations within the coma from reasonably high spatial resolution observations, emission flux gradients can be evaluated and these would directly lead to an improved understanding of the structure of the inner coma in terms of the neutrals and the dust. One of the earlier attempts in this direction was on Comet West (Bappu et al., 1980).

An extensive programme of observations of Comet Halley consisting of spectrophotometry, imaging photometry and astrometry were carried out in 1985 and 1986 using the telescopes at the Vainu Bappu Observatory, Kavalur of the Indian Institute of Astrophysics. Here, we report the results of our spectrophotometric observations viz., the fluxes in the emission bands and in the continuum derived therefrom as well as the distribution of fluxes as a function of the radial distance ($\varrho$) from the nucleus within the coma.

*Send offprint requests to*: K.R. Sivaraman

### 2. Observations

We observed the comet on 6 nights in November and December 1985 and on 11 nights in March, April, and May 1986. Our observations consisted of spectral scans with an automated spectrum scanner that used a thermoelectrically cooled RCA C31034 tube in the pulse counting mode at the $f/13$ cassegrain focus of the 102 cm reflector. The entrance aperture to the scanner was a circular diaphragm of 25″.9 in diameter and the exit slot had a band pass of 40 Å in the first order. With this, we obtained scans on the comet covering the range 4500–7200 Å on all the 3 nights of November and on Dec 20.570 and from 3900 to 6200 Å on the remaining nights except on April 17.694 where the scans extend upto 6700 Å. The telescope has an image scale of 15″.5 $mm^{-1}$ at the cassegrain focus and this large scale coupled with the 25″.9 diaphragm enabled us to sample different regions within the coma. We located this diaphragm on every night of observation at the brightest central part of the coma, namely the nucleus. In addition on 6 nights we systematically displaced the diaphragm to locations in the antisunward direction and on 3 nights to locations approximately normal to the sun-comet radius vector. Since one of the positions of the diaphragm every night was centred on the nucleus, all measurements of each night could be referred to this position. We have been able to observe regions out to as much as $\simeq 2'$ from the nucleus. These are schematically shown in Figs. 3 and 4 as insets. For each such position of the diaphragm, we scanned the neighbouring sky either before or after each scan on the comet and used this to eliminate the contribution of the background sky. We have then derived the energy distribution curves for all the scans on the comet following the reduction procedure described by Sivaraman et al. (1979) with the help of the observations of the standard stars $\theta$ Crt, 58 Aql, $\eta$ Hya, and 109 Vir. In Fig. 1 we show a sample of these curves for March 31.904 where the emission bands of $C_3(4050)$, $CH+CN(0,1)$, $C_2(1,0)$, $NH_2(0,13,0)$, $C_2(0,0)$, $C_2(0,1)$, and $C_2(2,4)$ are prominently seen.

We notice the presence of $NH_2(0,7,0)$ emission in our scans of November which extends till 7200 Å. $NH_2(0,13,0)$ emission can be marginally seen at 4900 Å in the November scans, but is definitely seen in the scans on Dec 8.813 and 19.576 although their flux is not significant. $NH_2(0,13,0)$ emission became unusually intense by March and is seen conspicuously in the scans of all the nights of March both at the nucleus as well as at locations away from the nucleus (Fig. 1). Since on these occasions our scans end at 6200 Å we have no way of checking the presence of $NH_2(0,7,0)$

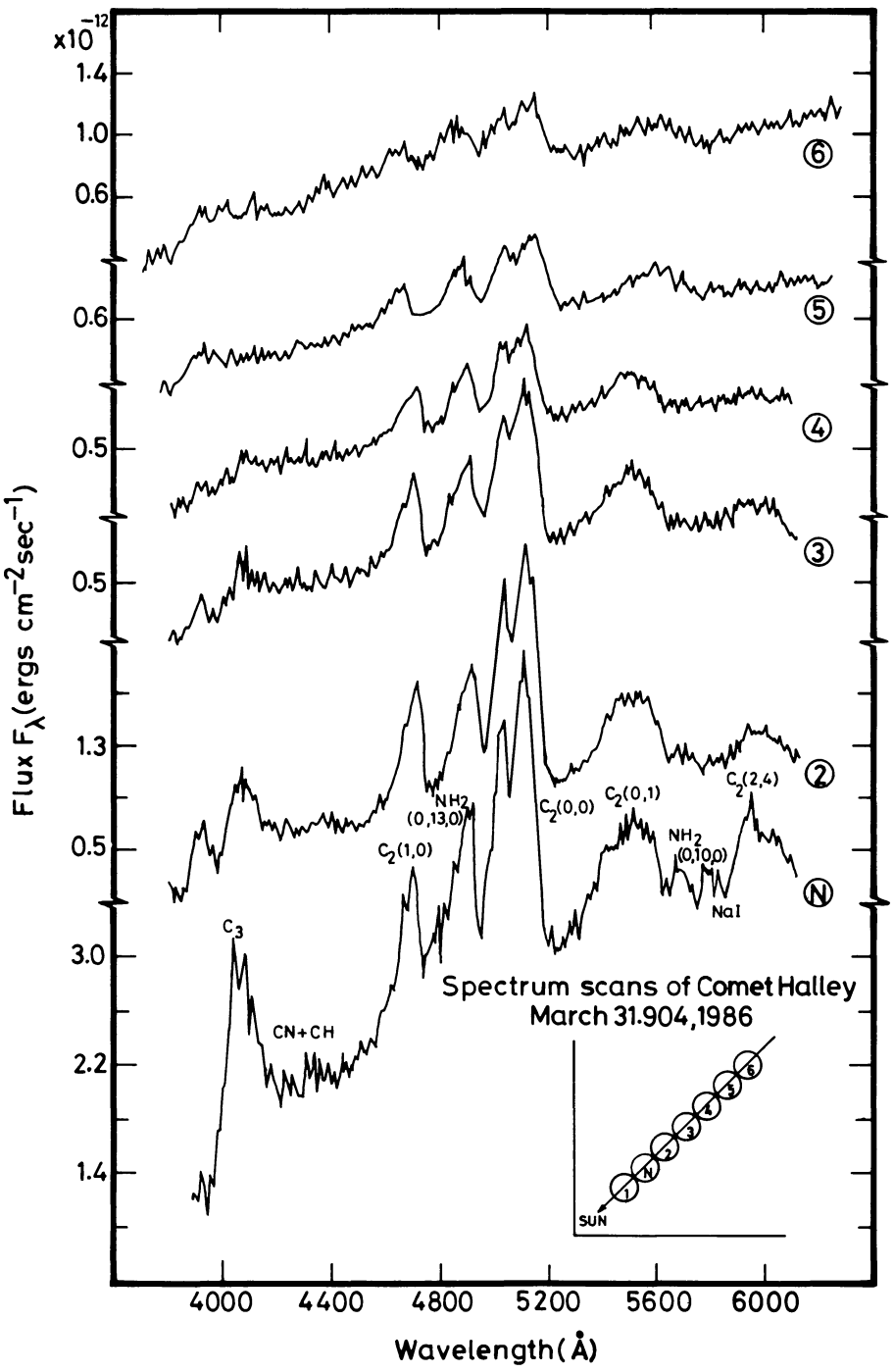


**Fig. 1.** Plot of flux $F_\lambda$ vs. wavelength corresponding to 6 locations (designated *N*, 2, 3 ... 6) of the 25″.9 diaphragm within the coma, *N* being the position of the nucleus. The 5 successive positions of the diaphragm (~28″ apart from each other) in the anti-sunward direction are schematically shown in the inset on the lower right corner. Notice the fast decrease in emission in the bands as the diaphragm is displaced systematically away from the nucleus

from our records. Again on April 17.694 when our scans extend upto 6700 Å, $NH_2(0,7,0)$ is seen well, but the flux in $NH_2(0,13,0)$ had decreased to the December level. Similarly $NH_2(0,10,0)$ emission is seen in all our records and on the nights of March is present significantly. Spectra of Arpigny et al. (1987) show all these bands of $NH_2$ clearly. Na I emission, although present in measurable quantities on the nights of March, is most likely to be contaminated by the bigger contribution from $NH_2(0,10,0)$. Since it may not be possible to separate the $NH_2$ emission from that of Na I reliably at the spectral resolutions we have employed, we have not attempted to calculate the fluxes of emission of Na I or $NH_2(0,10,0)$.

## 3. Results and discussion

### 3.1. *Emission band fluxes*

We have evaluated from these spectral energy curves, the fluxes in the emission bands of $C_3$, CN, CH, Swan bands, $NH_2$ and $H_2O^+$

**Table 1.** Observed emission band fluxes for the nucleus of comet P/Halley

| Date U.T. 1985-86 | r AU | Δ AU | Log F | | | | | | | | | | |
|---|---|---|---|---|---|---|---|---|---|---|---|---|---|
| | | | CN (λ3883) | $C_3$ (λ4050) | CN (λ4200) | CH (λ4350) | $C_2$(1,0) (λ4737) | $NH_2$(0,13,0) (λ4900) | $C_2$(0,0) (λ5165) | $C_2$(0,1) (λ5635) | $C_2$(2,4) (λ6050) | $NH_2$(0,7,0) (λ6600) | $H_2O^+$ (λ7050) |
| Nov. 16.904 | 1.71 | 0.72 | - | - | - | - | -10.91 | - | -10.66 | -11.02 | -11.01 | -11.31 | -10.62 |
| Nov. 17.748 | 1.69 | 0.71 | - | - | - | - | -10.93 | - | -10.64 | -11.04 | -11.30 | -11.01 | -10.70 |
| Nov. 18.762 | 1.68 | 0.69 | - | - | - | - | -10.90 | - | -10.65 | -11.03 | -11.33 | -11.06 | -10.74 |
| Dec. 8.813 | 1.38 | 0.70 | - | - | - | - | -10.83 | - | -10.66 | -10.97 | -11.27 | - | - |
| Dec. 19.576 | 1.21 | 0.90 | -10.92 | -10.39 | -11.21 | -11.32 | -10.30 | - | - 9.89 | -10.08 | -10.65 | - | - |
| Dec. 20.590 | 1.20 | 0.92 | -10.95 | -10.53 | -11.54 | -11.40 | -10.37 | - | - 9.84 | -10.07 | -10.51 | -10.85 | -11.04 |
| Mar. 21.918 | 1.00 | 0.79 | - | -10.03 | -10.64 | -10.68 | -10.09 | -10.12 | - 9.64 | - 9.80 | -10.34 | - | - |
| Mar. 23.950 | 1.04 | 0.74 | - | -10.21 | -11.05 | -11.02 | -10.21 | - 9.99 | - 9.68 | - 9.86 | -10.30 | - | - |
| Mar. 28.883 | 1.11 | 0.62 | - | - 9.69 | -10.47 | -10.95 | - 9.96 | - 9.82 | - 9.55 | - 9.72 | -10.15 | - | - |
| Mar. 29.896 | 1.13 | 0.59 | - | - 9.75 | -10.39 | -10.41 | - 9.70 | - 9.82 | - 9.27 | - 9.59 | -10.15 | - | - |
| Mar. 30.903 | 1.14 | 0.57 | - | -10.06 | -10.81 | -11.08 | -10.20 | -10.03 | - 9.73 | -10.03 | -10.38 | - | - |
| Mar. 31.904 | 1.16 | 0.55 | - | - 9.64 | -10.70 | -10.70 | - 9.90 | - 9.78 | - 9.39 | - 9.73 | -10.11 | - | - |
| Apr. 5.848 | 1.24 | 0.46 | - | - 9.70 | -10.35 | -10.40 | - 9.79 | - | - 9.54 | - 9.89 | -10.40 | - | - |
| Apr. 12.850 | 1.34 | 0.42 | - | - 9.59 | -10.29 | -10.35 | -10.00 | - | - 9.76 | - 9.87 | -10.22 | - | - |
| Apr. 17.694 | 1.42 | 0.47 | - | - 9.91 | -10.65 | -10.88 | -10.25 | - | -10.03 | -10.18 | -10.41 | -10.40 | - |
| Apr. 30.638 | 1.62 | 0.77 | - | -10.63 | -11.19 | -11.34 | -10.60 | - | -10.35 | -10.45 | -10.44 | - | - |
| May 7.622 | 1.72 | 0.99 | - | -10.83 | -11.06 | -11.02 | -10.73 | - | -10.60 | -10.82 | -11.16 | - | - |

r = heliocentric distance of comet in AU.

Δ = geocentric distance of comet in AU.

Log F = log of total flux in the emission band in ergs $cm^{-2}$ $s^{-1}$.

above the smoothed continuum level and also the flux in the continuum at 4860 Å. These are given in Table 1. We have then evaluated the total number of molecules ($N$) of each of these species contained in a cylinder of diameter 25″.9 in the line of sight and extending through the comet using the following relation which is valid for the resonance fluorescence mechanism (A'Hearn and Cowan, 1975).

$$N = L_i \frac{m_e \lambda_i}{\pi e^2 f \lambda_a p \varrho_v} = \frac{L_i}{g_i} \quad (1)$$

where

$L_i = 4\pi \Delta^2 F_\lambda$

$\Delta$ comet – earth distance in cm

$F_\lambda$ – band flux observed in the 26″ diaphragm

$\lambda_i$ – the mean wavelength of the emission band

$f$ – the oscillator strength

$p$ – the spontaneous transition probability from the upper to the lower level and

$\varrho_v$ – the solar radiation density at the site of the comet at the mean wavelength ($\lambda_a$) of absorption to the upper level.

The reciprocal of the coefficient of $L_i$ of Eq. (1) is represented by $g_i$ which is the fluorescence efficiency of the species for the emission band concerned. The values of $g_i$, adopted by us for the various bands are presented in Table 2. We have derived the efficiencies for the $C_2$(0,0) and $C_2$(0,1) sequences using the $C_2$(1,0) efficiency given by Oliversen et al. (1985) and the $C_2$ band sequence flux ratios given by A'Hearn (1978). We have used the $g$'s that are averaged over all the radial velocities of the comet. The values of the $g$'s when inserted in Eq. (1) lead to the following relations

**Table 2.** Fluorescence efficiency used for reduction of fluxes to column densities

| Species | Efficiency $g^*$ ergs $sec^{-1}$ | Source |
|---|---|---|
| $C_3$ | $1.5 \times 10^{-12}$ | [1] KSK |
| $C_2$(1,0) | $2.4 \times 10^{-13}$ | [2] Oliversen et al. |
| $C_2$(0,0) | $4.42 \times 10^{-13}$ | [3] A'Hearn |
| $C_2$(0,1) | $2.08 \times 10^{-13}$ | [3] A'Hearn |
| $NH_2$(0,7,0) | $1.75 \times 10^{-14}$ | [4] A'Hearn |
| $H_2O^+$ | $2.98 \times 10^{-12}$ | [5] Wycoff & Wehinger |

* Fluorescence efficiency per molecule at r = 1 AU.


1. Krishna Swamy, K.S. 1986, Personal Communication.
2. Oliversen, R.F., Hollis, J.M. and Brown, L.W., 1985, ICARUS, 63, 339.
3. A'Hearn, M.F. 1978, Astrophys. J. 219, 768.
4. A'Hearn, M.F., 1983, In 'Comets' ed. by L.Wilkening, University of Arizona Press, P.431.
5. Wycoff, S. and Wehinger, P.A., 1976, Astrophys. J. 204, 604.

**Table 3.** Column densities of molecules at the nucleus integrated over the radius $R$, i.e. total number of molecules in the observed column. $R$ is the projected radius of the 25″.9 diaphragm on the comet at the geocentric distances of observations

| Date U.T. 1985-86 | R in $10^4$ Km | Log N | | | | | |
|---|---|---|---|---|---|---|---|
| | | $C_3$ | $C_2(1,0)$ | $C_2(0,0)$ | $C_2(0,1)$ | $NH_2(0,7,0)$ | $H_2O^+$ |
| Nov. 16.904 | 0.67 | | 29.34 | 29.31 | 29.28 | 30.07 | 28.54 |
| Nov. 17.748 | 0.66 | | 29.29 | 29.32 | 29.25 | 30.35 | 28.43 |
| Nov. 18.762 | 0.65 | | 29.29 | 29.27 | 29.23 | 30.27 | 28.36 |
| Dec. 8.813 | 0.65 | | 29.20 | 29.11 | 28.13 | | |
| Dec. 19.576 | 0.84 | 28.94 | 29.83 | 29.98 | 30.12 | | |
| Dec. 20.590 | 0.86 | 28.82 | 29.78 | 30.05 | 30.14 | 30.43 | 28.02 |
| Mar. 21.918 | 0.74 | 29.02 | 29.77 | 29.95 | 30.12 | | |
| Mar. 23.950 | 0.69 | 28.83 | 29.63 | 29.89 | 30.04 | | |
| Mar. 28.883 | 0.58 | 29.25 | 29.78 | 29.92 | 30.08 | | |
| Mar. 29.896 | 0.55 | 29.16 | 30.01 | 30.18 | 30.19 | | |
| Mar. 30.903 | 0.53 | 28.82 | 29.49 | 29.70 | 29.72 | | |
| Mar. 31.904 | 0.51 | 29.23 | 29.77 | 30.02 | 30.00 | | |
| Apr. 5.848 | 0.43 | 29.07 | 29.79 | 29.77 | 29.75 | | |
| Apr. 12.850 | 0.39 | 29.17 | 29.56 | 29.54 | 29.76 | | |
| Apr. 17.694 | 0.44 | 29.00 | 29.47 | 29.42 | 29.59 | 30.45 | |
| Apr. 30.638 | 0.72 | 28.83 | 29.65 | 29.64 | 29.87 | | |
| May 7.622 | 0.93 | 29.39 | 29.80 | 29.66 | 29.77 | | |

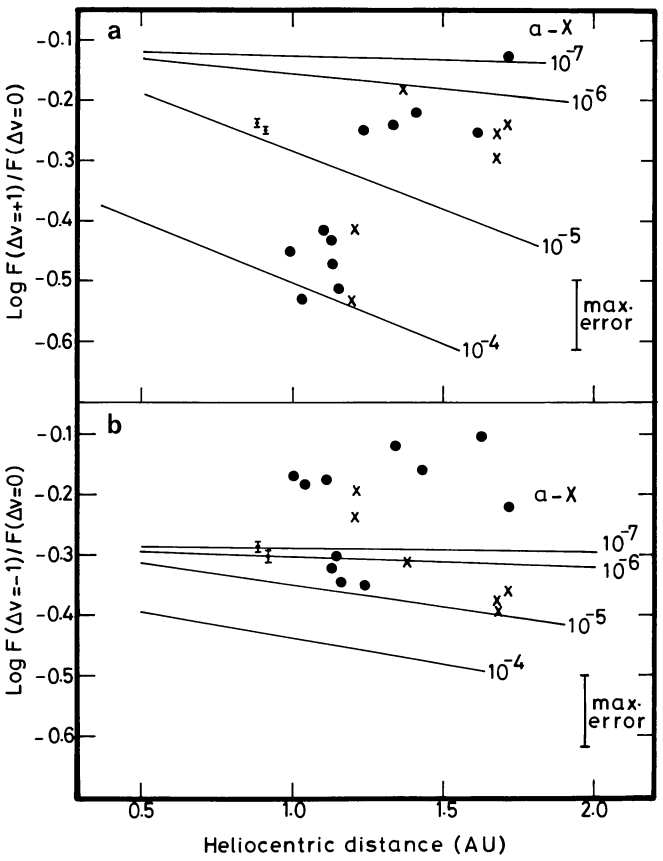


**Fig. 2. a** Swan band sequence flux ratio $\log F(\Delta V=+1)/F(\Delta V=0)$ as a function of heliocentric distance. Crosses: observations of pre-perihelion period; filled circles: observations of post-perihelion period. The solid lines are theoretical predictions reproduced here from Fig. 1 of O'Dell and Tegler (1987). **b** Same as Fig. 2a except for the $\log F(\Delta V=-1)/F(\Delta V=0)$ ratios. The solid lines are reproduced from Fig. 2 of O'Dell and Tegler (1987)

which we have used to derive the total number of molecules ($N$) of each species in the field of view.

$$\log N_{C_3} = \log F_\lambda + 2\log r\Delta + 39.262$$
$$\log N_{C_2(1,0)} = \log F_\lambda + 2\log r\Delta + 40.066$$
$$\log N_{C_2(0,0)} = \log F_\lambda + 2\log r\Delta + 39.80$$
$$\log N_{C_2(0,1)} = \log F_\lambda + 2\log r\Delta + 40.127$$
$$\log N_{NH_2(0,7,0)} = \log F_\lambda + 2\log r\Delta + 41.203$$
$$\log N_{H_2O^+} = \log F_\lambda + 2\log r\Delta + 38.972.$$

In Table 3 we have given the calculated values of the number of molecules ($N$) of each species for the position of the nucleus.

### 3.2. *Swan band sequence flux ratios*

The classical problem of the $C_2$ molecule has been the gross mismatch between the observed and theoretical band sequence flux ratios for the Swan bands based on resonance fluorescence mechanism (Stockhausen and Osterbrock, 1965; Mayer and O'Dell, 1968). Also, the vibrational temperature for the population distribution in the triplet levels needed to explain the observed intensities of the Swan bands were found to be discordant with the conditions prevailing in cometary atmospheres.

Krishna Swamy and O'Dell (1977, 1986) have constructed a model based on detailed fluorescence equilibrium calculations for $C_2$ including the Ballik-Ramsay bands, the Fox-Herzberg bands in addition to the Swan bands from which they predict the band sequence flux ratios and their dependence on the heliocentric distance of the comet. By comparing these theoretical values with the observed flux ratios, the efficacy of the model can be assessed. Recently O'Dell and Tegler (1987) have brought to light the discrepancy that exists between their observations on two occasions on Comet Halley and the theoretical predictions of the flux ratios based on this model. They find that, increasing the data points by pooling of similar observations from the literature for earlier comets does not bring down the discrepancy. Although, this would enhance the number of data points, the diversity existing in the different observations may not permit an impartial comparison, whereas it would be desirable to have a large number of observations on a single comet for this purpose. In this connection our flux ratios constitute a homogeneous set of observations obtained on a single comet using the same instrumentation. We have plotted the flux ratios $F(\Delta V=+1)/F(\Delta V=0)$ and $F(\Delta V=-1)/F(\Delta V=0)$ for all the nights of Table 1 onto Figs. 1 and 2 of O'Dell and Tegler (1987). These are shown in Figs. 2a and 2b. The discrepancies are obvious. It is surprising that even the sophisticated model for $C_2$ of Krishna Swamy and O'Dell is unable to resolve the discrepancy, thus leaving the problem of $C_2$ as enigmatic as ever.

### 3.3. *Emission profiles within the coma*

On 9 nights we obtained spectral scans at many locations within the coma, along and normal to the anti-sunward direction; both the directions passing through the nucleus. We have shown in Fig. 1 a set of traces of one night's observations. For all other similar sets of observations, we have followed the same reduction

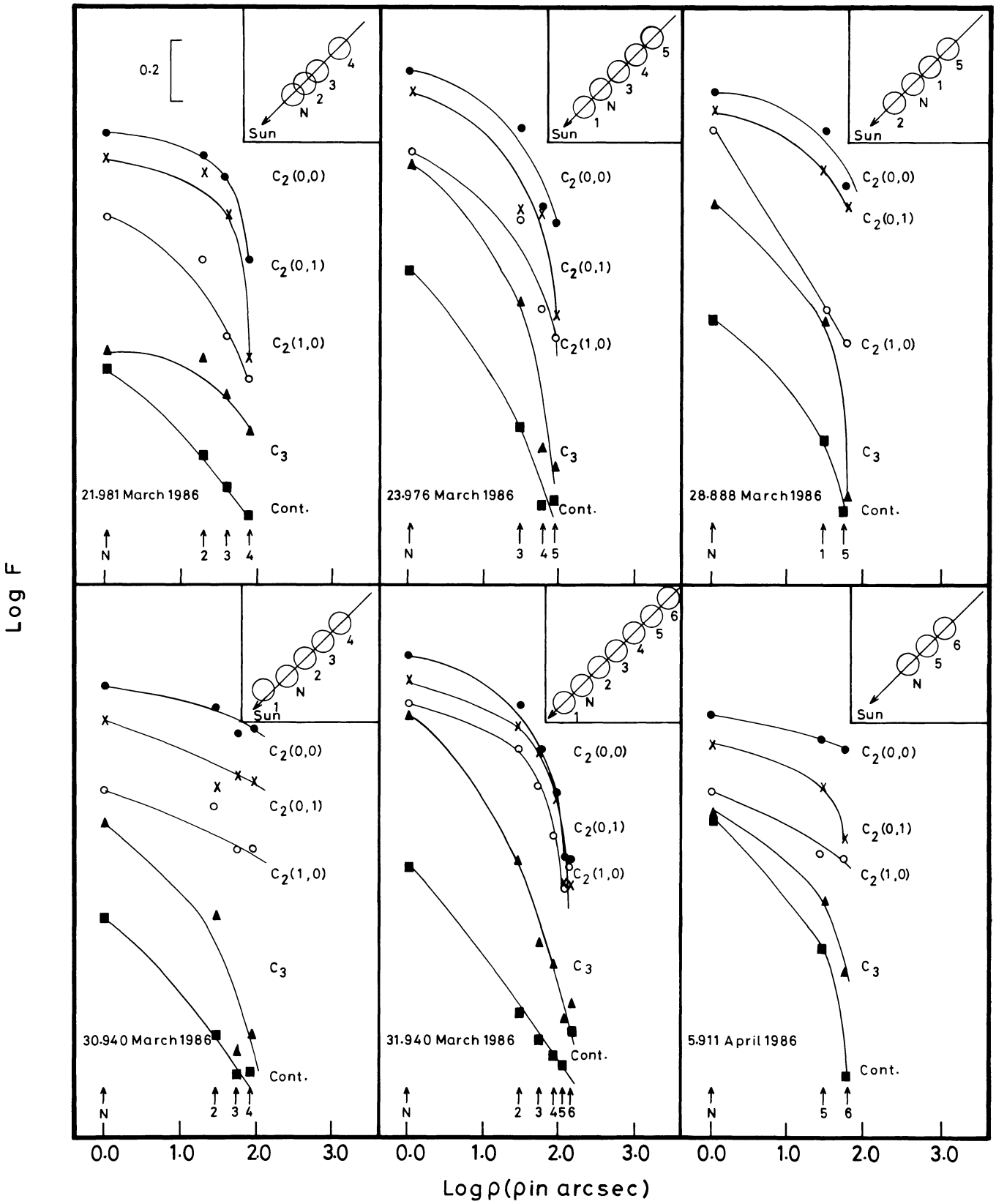


**Fig. 3.** Emission profiles for $C_3$, Swan bands and continuum as a function of the distance ($\varrho$) in arcsec of the centre of the diaphragm in the anti-sunward direction from the nucleus *N*. The positions of the diaphragm are schematically shown in the inset on the top right corner of each box and bearing designations *N*, 1, 2, 3 ... etc. as the case may be. These correspond to nucleus, positions 1, 2, 3 ... etc. and the same designations are reproduced on the *x*-axis in addition to the arcsec markings for convenience. Log of flux (log *F*) is along the *y*-axis. Within each box the profiles are shifted vertically to avoid overlap. The bar on the top left box represents 0.2 units in log *F*

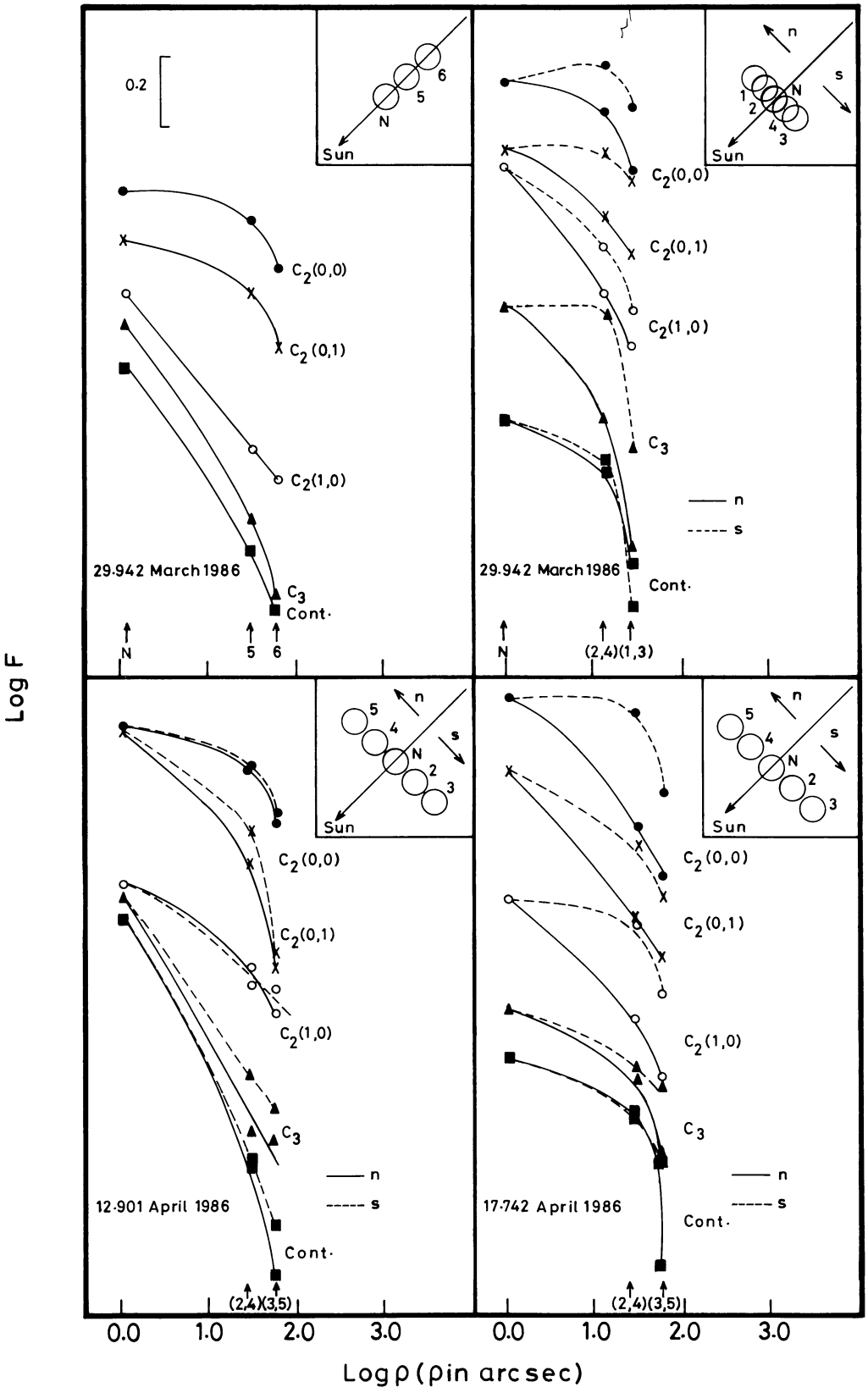


**Fig. 4.** Same as Fig. 3 except that the diaphragm positions are normal to the radius vector through the nucleus *N*. Notice that the emission profiles in the directions *n* (———) and *s* (– – – – –) are well separated bringing out the asymmetries. See text for details

**Table 4.** Dust-gas ratio for comet P/Halley for the nucleus

| Date U.T. 1985-86 | r AU | Phase angle in degrees | $F_{cont}(\lambda 4860)$ at $\Delta = 1$ AU (erg $s^{-1}$ $cm^{-2}$ $A^{-1}$) | $\frac{F_{cont\ (4000-6000)}}{F_{Swan\ bands}}$ | $\frac{F_{cont\ (4000-6000)}}{F_{C_3(4050)} + F_{Swan\ bands}}$ |
|---|---|---|---|---|---|
| Nov. 16.904 | 1.71 | 4.0 | $1.99 \times 10^{-13}$ | 18.81 | - |
| Nov. 17.748 | 1.69 | 2.4 | 3.03 | 27.49 | - |
| Nov. 18.762 | 1.68 | 1.4 | 2.43 | 23.23 | - |
| Dec. 8.813 | 1.38 | 42.9 | 1.52 | 16.62 | - |
| Dec. 19.576 | 1.21 | 53.3 | 2.51 | 2.61 | 2.26 |
| Dec. 20.590 | 1.20 | 53.7 | 3.68 | 4.11 | 3.71 |
| Mar. 21.918 | 1.00 | 66.1 | 6.29 | 4.45 | 3.72 |
| Mar. 23.950 | 1.04 | 65.8 | 4.98 | 4.73 | 4.11 |
| Mar. 28.883 | 1.11 | 62.8 | 7.60 | 6.96 | 5.14 |
| Mar. 29.896 | 1.13 | 61.8 | 7.43 | 6.35 | 5.39 |
| Mar. 30.903 | 1.14 | 60.5 | 3.94 | 7.06 | 5.64 |
| Mar. 31.904 | 1.16 | 59.1 | 7.57 | 7.42 | 5.62 |
| Apr. 5.848 | 1.24 | 49.1 | 5.60 | 9.14 | 6.79 |
| Apr. 12.850 | 1.34 | 29.1 | 4.45 | 12.26 | 7.56 |
| Apr. 17.694 | 1.42 | 21.1 | 4.42 | 19.97 | 12.27 |
| Apr. 30.638 | 1.62 | 28.4 | 1.90 | 8.39 | 6.85 |
| May 7.622 | 1.72 | 30.8 | 0.40 | 28.35 | 15.87 |

procedure as for the scan on the nucleus and have obtained the flux ($F_\lambda$) in the emission bands. Using these, we have constructed the emission profiles for $C_3$, Swan bands of $C_2$ and the continuum at 4860 Å, which are plots of $\log F_\lambda$ vs. $\log \varrho$, $\varrho$ being the distance of the centre of the diaphragm in arcsecs from the nucleus. These emission profiles are shown in Figs. 3 and 4.

The emission profiles along the radius vector show that, on the same night the three bands of $C_2$ show the same gradients while the profiles of $C_3$ and continuum are generally steeper. All the profiles of March 23.976 and 31.948 are steeper than their counterparts of the remaining nights showing that, there are nightly variations. These are possibly due to minor explosions in the nucleus resulting in changes in the gradients from an average value. The dust profiles also show similar variations and this cannot be completely attributed to changes in phase angle, which are small in this short span of time.

Of greater interest is the behaviour of the gradients normal to the radius vector. The diaphragm positions lying above the radius vector are designated as direction *n* and those below this line as direction *s* for the sake of the present discussion. On March 29.942 we have profiles along the radius vector as well as normal to it. These show that the gradients are steeper in the normal direction than along the radius vector for $C_2$, while for $C_3$ and continuum the reverse is true. Further, the gradients along the directions *n* and *s* also widely differ from each other. These asymmetries are most prominent in the $C_2$ profiles of March 29.942 and April 17.742. The continuum is symmetrical in *n* and *s* directions. The asymmetries in the distribution of the neutrals and dust within the coma of Halley seem to be also time dependent. We propose to discuss these in greater detail in terms of the production rates in our next paper.

### *3.4. Dust-gas ratio*

We have computed the ratios of the fluxes in the continuum over the range 4000–6000 Å to the sum of the fluxes in the Swan bands on all nights. This ratio may serve as an indicator of the dust-gas ratio in comets. But in the case of Comet Halley $C_3$(4050 Å) emission was quite strong in the spectrum and we have added its contribution to those of the Swan bands while calculating the ratio. Ideally, the CN(0,0) band flux and those of CH, $NH_2$, $H_2O^+$ should also have been included. Our spectra do not reach the CN(0,0) band and the other bands are rather weak and may not alter the ratios significantly. We have presented these ratios in Table 4, where we have included the heliocentric distances (*r*) and the phase angle values ($\phi$). The ratio decreased fast from November 16.904 ($r = 1.71$ AU) towards December 20.590 ($r = 1.20$ AU). After perihelion, the ratio increased steadily from March 21.918 ($r = 1.0$ AU) to May 7.622 ($r = 1.72$ AU). This behaviour of the ratio is consistent with the scenario that, as the comet approaches the Sun, the grains undergo sputtering by UV radiation as well as solar wind and are broken up into fine particles whose net contribution to the continuum flux can be expected to go down. In the vicinity of the Sun, as the grains evaporate or are destroyed, the gaseous component is likely to increase and so also the emission in the bands. Thus the ratio of the flux in the continuum to that in the emission bands will be further reduced. After perihelion passage, the grains will start growing and therefore the trend will be reversed as shown in our Table 4. The influence due to changes in phase angle appears to be secondary, when compared to that of the heliocentric distance parameter.

## 4. Conclusions

1. The fluxes in the emission bands derived from the energy distribution curves for 17 nights (Table 1) show the time dependent evolution in the pre and post perihelion periods.

2. The Swan band-sequence flux ratios $F(\Delta V = +1)/F(\Delta V = 0)$ and $F(\Delta V = -1)/F(\Delta V = 0)$ obtained from our observations do

not match with the ratios predicted by the model for $C_2$ emission by Krishna Swamy and O'Dell (1977) (Figs. 2a and b).

3. The emission profiles in $C_3$, Swan bands and the continuum obtained from the spatial scans show varying gradients for the different species. These seem to change with time and also exhibit spatial asymmetries (Figs. 3 and 4).

*Acknowledgements.* The authors are thankful to Prof. J.C. Bhattacharyya, Director, Indian Institute of Astrophysics for the kind encouragement and for providing graciously telescope time and to the Department of Space, for partial fincancial support. The valuable help by K. Kuppuswamy, M.J. Rozario, and K. Jayakumar at the telescope and by R. Kariyappa and J.S. Nathan in the computations are gratefully acknowledged. We are thankful to G.A. Shah for reading through the manuscript and for his suggestions.

**References**

A'Hearn, M.F., Cowan, J.J.: 1975, *Astron. J.* **80**, 852
A'Hearn, M.F.: 1978, *Astrophys. J.* **219**, 768
Arpigny, C., Dossin, F., Zucconi, J.M., Andrillat, Y., Manfroid, F., Hutsemekers, D.: 1987, Proc. 20th ESLAB Symposium on *Exploration of Halley's Comet*, ESA SP-250, p. 471
Bappu, M.K.V., Parthasarathy, M., Sivaraman, K.R., Babu, G.S.D.: 1980, *Monthly Notices Roy. Astron. Soc.* **192**, 641
Krishna Swamy, K.S., O'Dell, C.R.: 1977, *Astrophys. J.* **216**, 158
Krishna Swamy, K.S., O'Dell, C.R.: 1986, *Astrophys. J.* (submitted) (personal communication)
Mayer, P., O'Dell, C.R.: 1968, *Astrophys. J.* **153**, 951
O'Dell, C.R., Tegler, S.C.: 1987, Proc. 20th ESLAB Symposium on *Exploration of Halley's Comet*, ESA SP-250, p. 561
Oliversen, R.J., Hollis, J.M., Brown, L.W., 1985, *Icarus*, **63**, 339
Sivaraman, K.R., Babu, G.S.D., Bappu, M.K.V., Parthasarathy, M.: 1980, *Monthly Notices Roy. Astron. Soc.* **189**, 897
Stockhausen, R.E., Osterbrock, D.E., 1965, *Astrophys. J.* **141**, 287